Volume 24, No 3 | International Journal of Radiation Research, July 2026

Value of a model combining clinical indicators with qualitative and quantitative contrast-enhanced ultrasound parameters for differentiating benign and malignant prostatic lesions

L. Yu, F. Shen, X. Chen, L. Han, Y. Qiu*

Department of Ultrasound, Haining Central Hospital, Haining, China

► ***Original article***

Corresponding author:
Yun Qiu, B.M.,
E-mail:
qiuyun94028455@163.com

Received: April 2026
Final revised: May 2026
Accepted: May 2026

Int. J. Radiat. Res., July 2026; 24(3): 735-740

DOI: 10.61186/ijrr.24.3.21

Keywords: *Prostatic neoplasms, ultrasonography, contrast media, prostate -specific antigen, differential diagnosis.*

ABSTRACT

Background: Benign prostate lesions and cancer can be difficult to separate when the judgment depends on one test only, this study reviewed routine clinical data, visual CEUS signs, and measured CEUS blood-flow values, then combined useful items in a simple prediction model. ***Materials and Methods:*** We reviewed 120 patients from one hospital, all had pathological proof of a prostate lesion and underwent transrectal ultrasound plus CEUS between January 2021 and December 2025; clinical indexes, image signs, and curve-based CEUS values were checked in benign and malignant cases, related variables were screened with logistic regression, and ROC analysis together with bootstrap resampling was used for model checking. ***Results:*** The malignant cases showed an unfavorable PSA pattern and abnormal DRE more often than benign cases, on CEUS they also had more hyperenhancement, uneven enhancement, early wash-in, and perfusion defects; the curve data suggested quicker and stronger enhancement. In the adjusted analysis, f/tPSA, PSAD, early wash-in, and PI remained related to cancer. The model reached an AUC of 0.930, with sensitivity of 82.2% and specificity of 89.3%; the corrected AUC after bootstrap testing was 0.918. ***Conclusion:*** Putting clinical indexes together with visual and numerical CEUS information gave a useful and internally stable way to separate benign prostate lesions from malignant ones.

INTRODUCTION

Prostate lesions are common among men in middle and old age, and doctors often need to decide whether a lesion is likely to be benign or cancerous before choosing biopsy, observation, or treatment [1-4]. PSA testing and DRE are still used in the first assessment, but either test alone is not very specific; benign hyperplasia, infection or inflammation, and a large gland can all raise suspicion even without cancer [5-9]. Because of this problem, current risk judgment usually puts several pieces of evidence together, including PSA-related numbers, physical examination, imaging results, and pathology when available [5, 9].

Transrectal ultrasound is a common examination because it is direct, available in many hospitals, and useful when doctors need to locate a lesion or guide biopsy [10,11]. Its weakness is also clear, since conventional ultrasound mainly describes the shape and echo of the prostate; it does not show small-vessel perfusion well, and some early or nearly isoechoic cancers may not be obvious [12, 13]. CEUS adds dynamic information after microbubble injection, so the examiner can watch how contrast enters and leaves the lesion; cancer may show strong enhancement, uneven filling, early entry of contrast, quick wash-out, or small areas with poor perfusion [14-17].

CEUS can also be analyzed with time-intensity curves. The common values include AT, TTP, PI, MTT, wash-in slope, and AUC, and these values give a more measurable description of the enhancement process [18, 19]. However, benign and malignant lesions do not always look clearly different. Inflammation and hyperplastic nodules may have rich focal blood flow, while cancer can vary with tumor grade, size, and necrotic change [20-22]. For this reason, a single sign from clinical examination or CEUS is often not enough for a dependable decision.

Recent prostate imaging studies have therefore placed more weight on multi-index assessment and risk grouping [23-25]. Even so, fewer studies have put routine clinical variables, visual CEUS features, and quantitative CEUS curve values into one model, and some reports did not show calibration results. The present study tried to join these three kinds of information in a logistic model that clinicians can still understand, then we tested both its discrimination and its internal stability. The aim was to find variables linked with malignancy and to offer a simple aid for diagnosis and risk assessment.

[Downloaded from ijrr.com on 2026-11-15]

[DOI: 10.66224/ijrr.24.3.21]

MATERIALS AND METHODS

Study Population

We screened consecutive patients treated in our hospital from January 2021 to December 2025. The study included only patients who had a prostate lesion and had finished both transrectal conventional ultrasound and CEUS.

Patients were included when they met all of the following points: (1) age at least 18 years; (2) transrectal conventional ultrasound and CEUS performed because PSA was high, DRE was abnormal, or another imaging test suggested a prostate lesion; (3) pathology obtained within 2 weeks after CEUS, by systematic biopsy with targeted biopsy under transrectal ultrasound guidance, transurethral resection, or radical prostatectomy; (4) clinical records, CEUS images, and pathological results were complete; and (5) the images were clear enough for review.

Patients were not kept in the analysis if any of these conditions were present: (1) previous prostate operation, radiotherapy, endocrine treatment, or other treatment that could change local perfusion; (2) poor CEUS recording or missing image data, so that curve values could not be taken; (3) absence of important clinical indexes; (4) pathology that did not give a clear result; or (5) an interval of more than 2 weeks between CEUS and tissue sampling.

After screening, 120 patients were available for analysis, with 75 benign lesions and 45 malignant lesions.

Collection of clinical data

We obtained the clinical and laboratory data from the electronic medical record system. The collected items were age, tPSA, fPSA, f/tPSA, prostate volume, PSAD, and DRE result. The prostate volume came from three diameters measured by transrectal ultrasound, namely anteroposterior, transverse, and craniocaudal diameters. We used the ellipsoid formula, prostate volume (mL) = anteroposterior diameter × transverse diameter × craniocaudal diameter × 0.52. PSAD was tPSA (ng/mL) divided by prostate volume (mL). DRE was recorded as abnormal or not obviously abnormal; nodules, a hard gland, or fixation were treated as abnormal findings.

Ultrasound examination

One physician completed all ultrasound examinations, and this physician had more than 10 years of experience with prostate ultrasound. We used a Logiq E9 color Doppler system and an endorectal probe (GE Healthcare, Milwaukee, WI, USA). The probe worked at 4-9 MHz. Conventional ultrasound, CEUS mode, and the built-in quantitative software were available on the machine. The contrast agent was SonoVue, which contains sulfur hexafluoride microbubbles (Bracco Suisse SA, Plan-les-Ouates, Switzerland).

Before the scan, patients were asked to empty the rectum partly, and they lay in the left lateral position. Conventional transrectal ultrasound was performed first, mainly for prostate size, shape, capsule, internal echo, and suspected lesions. After that, the machine was switched to CEUS. A 1.5 mL bolus of SonoVue was given through the cubital vein, then 5 mL saline was injected, and dynamic recording began at the same time. The lesion and surrounding prostate tissue were watched for at least 120 s. The examiner tried to keep the probe position and pressure stable, because pressure changes could affect local perfusion. All cine loops were stored as DICOM files for later offline measurement.

CEUS image analysis

Two ultrasound doctors, both with more than 5 years of experience in prostate CEUS, reviewed the images separately. They did not know the clinical information or the pathological diagnosis. When their readings were not the same, they discussed the case and reached one final result. The recorded visual CEUS signs were hyperenhancement, heterogeneous enhancement, early wash-in, rapid wash-out, unclear margin, and perfusion defect.

For the numerical part, the dynamic CEUS clips were opened in the built-in software. The ROI was drawn manually on the image plane where the lesion enhanced most clearly, and the ROI covered as much of the lesion as possible. Calcification, necrotic or cystic areas, and large vessels were avoided. Another ROI with a similar setting was placed in nearby normal prostate tissue. The software produced the time-intensity curves, from which AT, TTP, PI, wash-in slope, MTT, and AUC were taken. We used the same ROI rule and the same workflow in every case to keep measurement differences as low as possible. Figure 1 gives example CEUS images.

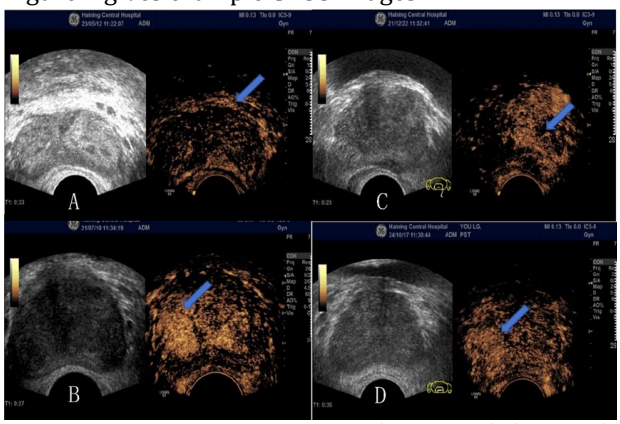


Figure 1. Representative conventional transrectal ultrasound and contrast-enhanced ultrasound images of malignant and benign prostatic lesions. **(A, B)** Prostate cancer showing rapid and marked arterial-phase hyperenhancement. **(C)** Prostatitis showing focal rapid arterial-phase hyperenhancement. **(D)** Benign prostatic lesion showing focal rapid arterial-phase hyperenhancement. Left images are conventional ultrasound; right images are contrast-enhanced ultrasound. Arrows indicate the target lesions or regions of interest.

[Downloaded from ijrr.com on 2026-11-15]

[DOI: 10.66224/ijrr.24.3.21]

Reference standard

Pathology was taken as the final standard. Tissue was collected according to the clinical need, by transrectal ultrasound-guided systematic biopsy with targeted biopsy, transurethral resection of the prostate, or radical prostatectomy. The samples were fixed in 10% neutral buffered formalin, then processed, embedded in paraffin, and cut into 4 um slices with a microtome (Leica Biosystems, Wetzlar, Germany). H&E staining was done by routine laboratory methods, and the slides were examined with a light microscope (Olympus Corporation, Tokyo, Japan).

Two pathologists with experience in prostate diagnosis read the slides independently, and they did not know the CEUS findings. Malignant lesions were prostate adenocarcinoma proved by pathology. Benign lesions covered benign prostatic hyperplasia, chronic prostatitis, and other non-cancer changes. If the two pathologists gave different opinions, they reviewed the slides together and made a consensus diagnosis. Figure 2 shows representative pathological images.

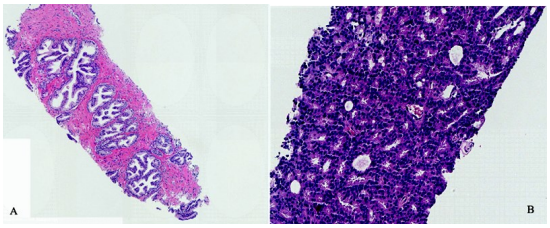


Figure 2. Representative histopathological photomicrographs of benign and malignant prostatic lesions. **(A)** Benign prostatic lesion showing benign glandular hyperplasia/chronic inflammatory changes. **(B)** Malignant prostatic lesion showing adenocarcinoma. Hematoxylin-eosin staining; original magnification: A, ×100; B, ×200.

Statistical analysis

Data analysis was done with SPSS 26.0 (IBM Corp., Armonk, NY, USA), R 4.3.1 (R Foundation for Statistical Computing, Vienna, Austria), and PASS 15.0 (NCSS, LLC, Kaysville, UT, USA). For continuous data, we used mean +/- standard deviation when the distribution was roughly normal, otherwise median and interquartile range were used. The independent-samples t test or the Mann-Whitney U test was chosen as suitable. Count data were written as number with percentage, and were checked with the chi-square test or Fisher exact test. Variables associated with malignant lesions in the single-factor analysis were considered for logistic regression, after collinearity was checked. ROC analysis was used to describe discrimination, and 1,000 bootstrap samples were used to examine internal stability. $P < 0.05$ on two-sided testing was regarded as significant.

RESULTS

Comparison of general clinical characteristics

The clinical comparison is listed in table 1. Patients in the malignant group were older, and their PSA-related results looked more suspicious. This group had higher tPSA and PSAD, lower f/tPSA, smaller prostate volume, and a higher rate of abnormal DRE findings, with all *P* values no more than 0.036. fPSA alone was not significantly different between groups (*P*=0.130).

Table 1. Clinical characteristics of patients with benign and malignant prostatic lesions.

Variable	Benign Group (n = 75)	Malignant Group (n = 45)	Statistic	P Value
Age (years)	66.5 ± 6.6	69.3 ± 7.0	t = -2.13	0.036
tPSA (ng/mL)	10.20 (7.42, 14.12)	15.92 (12.25, 22.89)	U = 837.00	<0.001
fPSA (ng/mL)	1.76 (1.23, 2.40)	1.96 (1.37, 2.93)	U = 1408.00	0.13
f/tPSA	0.176 ± 0.045	0.129 ± 0.040	t = 5.95	<0.001
Prostate volume (mL)	53.0 ± 13.7	43.4 ± 11.0	t = 4.20	<0.001
PSAD	0.20 (0.14, 0.29)	0.36 (0.30, 0.54)	U = 635.00	<0.001
Abnormal DRE, n (%)	15 (20.0)	20 (44.4)	x^2 = 6.99	0.008

Data are presented as mean ± standard deviation, median (interquartile range), or n (%). P values represent comparisons between the benign and malignant groups. Independent-samples t test was used for normally distributed variables, Mann-Whitney U test for non-normally distributed variables, and x2 test for categorical variables. tPSA, total prostate-specific antigen; fPSA, free prostate-specific antigen; f/tPSA, free-to-total prostate-specific antigen ratio; PSAD, prostate-specific antigen density; DRE, digital rectal examination.

Comparison of qualitative CEUS imaging features

Table 2 presents the visual CEUS findings. Hyperenhancement, heterogeneous enhancement, early wash-in, and perfusion defects were seen more often in malignant lesions, and all of these comparisons were significant (all $P \leq 0.016$). Rapid wash-out and unclear margin were also more common in the malignant group, but these two differences did not reach statistical significance (P=0.119 and P=0.083).

Table 2. Qualitative contrast-enhanced ultrasound features in benign and malignant prostatic lesions.

Variable	Benign Group (n = 75)	Malignant Group (n = 45)	Statistic	P Value
Hyperenhancement, n (%)	30 (40.0)	29 (64.4)	x^2 = 5.78	0.016
Heterogeneous enhancement, n (%)	24 (32.0)	28 (62.2)	x^2 = 9.27	0.002
Early wash-in, n (%)	25 (33.3)	30 (66.7)	x^2 = 11.28	<0.001
Rapid wash-out, n (%)	36 (48.0)	29 (64.4)	x^2 = 2.44	0.119
Unclear margins, n (%)	25 (33.3)	23 (51.1)	x^2 = 3.00	0.083
Perfusion defects, n (%)	11 (14.7)	18 (40.0)	x^2 = 8.52	0.004

Data are presented as n (%). P values were calculated using the χ^2 test. CEUS, contrast-enhanced ultrasound.

Comparison of quantitative CEUS parameters

The quantitative CEUS values are given in table 3. Compared with benign lesions, malignant lesions showed earlier and stronger enhancement, with shorter AT, TTP, and MTT, and higher PI, wash-in slope, and AUC (all $P \leq 0.037$).

Univariable and multivariable logistic regression analyses

Table 4 shows the regression results. In the

[Downloaded from ijrr.com on 2026-11-15]

[DOI: 10.66224/ijrr.24.3.21]

univariable analysis, malignant lesions were associated with age, f/tPSA, PSAD, hyperenhancement, heterogeneous enhancement, early wash-in, perfusion defects, AT, PI, MTT, and AUC (all P<0.05). After adjustment, four variables remained in the model: f/tPSA, PSAD, early wash-in, and PI.

Table 3. Quantitative contrast-enhanced ultrasound perfusion parameters in benign and malignant prostatic lesions.

Variable	Benign Group (n = 75)	Malignant Group (n = 45)	Statistic	P Value
AT (s)	13.79 ± 1.72	12.28 ± 1.72	t = 4.66	<0.001
TTP (s)	24.85 ± 2.96	23.60 ± 2.43	t = 2.50	0.014
PI (dB)	19.05 ± 2.61	20.96 ± 2.23	t = -4.27	<0.001
Wash-in slope	1.24 ± 0.27	1.48 ± 0.33	t = -4.12	<0.001
MTT (s)	33.52 ± 4.30	30.71 ± 3.18	t = 4.09	<0.001
AUC	804.00±112.05	850.90±120.58	t = -2.12	0.037

Data are presented as mean ± standard deviation. P values were calculated using the independent-samples t test. CEUS, contrast-enhanced ultrasound; AT, arrival time; TTP, time to peak; PI, peak intensity; MTT, mean transit time; AUC, area under the curve.

Table 4. Univariable and multivariable logistic regression analyses of factors associated with malignant prostatic lesions.

Variable	Univariable OR (95% CI)	P Value	Multivariable OR (95% CI)	P Value
Age (per 1-year increase)	1.064 (1.004-1.127)	0.035	-	-
f/tPSA (per 0.01 increase)	0.772 (0.692-0.861)	<0.001	0.714 (0.607-0.839)	<0.001
PSAD (per 0.1 increase)	2.137 (1.537-2.972)	<0.001	2.305 (1.511-3.516)	<0.001
Hyperenhance-ment (yes vs. no)	2.719 (1.265-5.845)	0.01	-	-
Heterogeneous enhancement (yes vs. no)	3.500 (1.615-7.587)	0.002	-	-
Early wash-in (yes vs. no)	4.000 (1.826-8.761)	<0.001	9.470 (2.650-33.838)	<0.001
Perfusion defects (yes vs. no)	3.879 (1.618-9.301)	0.002	-	-
AT (per 1-s increase)	0.592 (0.457-0.766)	<0.001	-	-
PI (per 1-dB increase)	1.382 (1.162-1.644)	<0.001	1.369 (1.063-1.762)	0.015
MTT (per 1-s increase)	0.827 (0.743-0.922)	<0.001	-	-
AUC (per 1-unit increase)	1.004 (1.000-1.007)	0.036	-	-

Odds ratios are presented with 95% confidence intervals. Variables entered into multivariable analysis were selected based on univariable significance, clinical relevance, and lack of substantial collinearity. OR, odds ratio; CI, confidence interval; PSAD, prostate-specific antigen density; AT, arrival time; PI, peak intensity; MTT, mean transit time; AUC, area under the curve.

Discriminative performance and internal validation of the combined model

The final model used f/tPSA, PSAD, early wash-in, and PI, and the equation was:

Logit(*P*) = -5.477 - 0.337 × (each 0.01 increase in f/tPSA) + 0.835 × (each 0.1 increase in PSAD) + 2.248 × (early wash-in) + 0.314 × PI

Here, early wash-in was entered as 0 for no and 1 for yes, while P indicated the estimated probability of malignancy. The ROC curve gave an AUC of 0.930 (95% CI: 0.883-0.968). With 0.432 as the selected cutoff, the sensitivity was 82.2%, the specificity was 89.3%, and the accuracy was 86.7%. Bootstrap testing showed only small optimism (0.012), and the corrected AUC was 0.918. The calibration result was acceptable, with a Hosmer-Lemeshow P value of 0.734 and a Brier score of 0.103.

DISCUSSION

This study asked whether simple clinical information and CEUS findings could be used together when judging benign and malignant prostate lesions. The adjusted analysis kept four items in the final model, namely f/tPSA, PSAD, early wash-in, and PI. With these items, the model showed good separation ability, reasonable calibration, and stable results in internal checking. The finding is consistent with daily practice, because doctors rarely depend on one result alone; PSA-related indexes, visual CEUS signs, and measured perfusion values are more useful when they are considered at the same time [14, 15, 17, 18, 23-25].

For the clinical indexes, PSAD and f/tPSA were more useful than tPSA after adjustment. This result is not surprising. tPSA may increase in benign prostatic hyperplasia, prostatitis, urinary retention, and other non-cancer states, so its specificity is limited [5, 9, 12]. PSAD partly corrects this problem by taking prostate size into account. f/tPSA describes the proportion of different PSA forms in blood, and it has been used for a long time in men suspected of having prostate cancer [12,23]. Keeping both indexes in the model suggests that they add different information, rather than repeating the same message.

The CEUS results also matched the expected blood-flow changes in cancer. Malignant lesions more often had hyperenhancement, heterogeneous enhancement, early wash-in, and perfusion defects. Their curve values also showed shorter AT, TTP, and MTT, with higher PI, wash-in slope, and AUC. These changes may be related to tumor angiogenesis, immature vessels, and abnormal microcirculation [14-18]. Among the visual signs, only early wash-in remained after adjustment. This means that a quick visual entry of contrast may be a useful sign of malignant vascular change. Earlier CEUS studies also reported that prostate cancers often enhance earlier and more strongly than benign tissue [17-20].

PI was the only measured perfusion value that stayed independently related to malignancy. Time-related values may be affected by several hemodynamic factors at once, but PI mainly reflects the highest enhancement level, so it is closer to the intensity of local blood supply [18-20]. The other CEUS values should not be viewed as meaningless only because they were not retained in the adjusted model. Some of them may overlap with PI or early wash-in, and some may lack specificity because inflammation and hyperplastic nodules can also show uneven or

[Downloaded from ijrr.com on 2026-11-15]

[DOI: 10.66224/ijrr.24.3.21]

rich enhancement [20-22].

A useful feature of this work is that it did more than compare benign and malignant groups. It built a model that can be read and used without complex black-box methods. In actual clinical work, physicians usually combine serum markers, examination findings, and imaging signs before deciding whether a lesion is suspicious. The model in this study follows that habit, because it contains two laboratory indexes, one visual CEUS sign, and one curve-based perfusion value. Its AUC of 0.930 suggests that the combined approach has practical value. This agrees with previous studies in which multi-parameter models performed better than single-method assessment for prostate disease [23-25]. A similar idea was also seen in an IJRR report, where MRI features used together helped separate prostatitis, benign prostatic hyperplasia, and prostate cancer [26].

This study also included internal validation and calibration, which are sometimes absent in diagnostic papers. Bootstrap resampling showed low optimism, and the corrected AUC remained high. The Hosmer-Lemeshow test and Brier score also suggested that predicted probabilities were reasonably close to observed results. These findings make the model more convincing as an auxiliary tool, although pathology remains the final basis for diagnosis [7,24].

Several limitations should be noted. The study was retrospective and came from one center, and the sample size was not large, so selection bias is possible. The model was checked internally only, and its performance in other hospitals, patient groups, operators, and ultrasound systems are still unknown. Benign and malignant lesions were also confirmed through different sampling methods, and biopsy can miss part of a lesion. In addition, malignant cases were not divided by Gleason score, tumor burden, or stage, and MRI or other imaging data were not added. Although CEUS and pathology images were included as examples, ROI drawing and image acquisition still need better standardization in later work.

In general, both clinical indexes and CEUS perfusion features contributed to the separation of benign and malignant prostate lesions. The model including f/tPSA, PSAD, early wash-in, and PI may help with auxiliary diagnosis and biopsy decisions. Larger prospective studies from several centers are needed to test this model outside the present hospital and to see how much it adds when MRI or new biomarkers are also used.

CONCLUSION

Benign and malignant prostate lesions differed in clinical indexes and CEUS perfusion findings. f/tPSA, PSAD, early wash-in, and PI were independent factors linked with malignant lesions. The combined model showed good discrimination, stable internal performance, and acceptable calibration; it may serve as a reference for risk grading and auxiliary diagnosis. Before wider clinical use, prospective multicenter studies and external validation are still needed.

***Conflict of Interests*:** The authors declared no conflict of interest.

***Funding*:** Not applicable.

***Ethical consideration*:** The Ethics Committee of Haining Central Hospital approved this retrospective diagnostic study (Approval No. HCH-EC-2023-147; approval date: January 20, 2023). The committee waived written informed consent because the work used retrospective data. The study followed the Declaration of Helsinki.

***Acknowledgments*:** The authors thank the Department of Ultrasound and the Department of Pathology of Haining Central Hospital for support in data collection and pathological review.

Authors' Contributions: Y.Q. designed and supervised the study. L.Y. and F.S. collected clinical and imaging data. X.C. and L.H. reviewed the images and performed data analysis. L.Y. wrote the first draft. All authors revised the paper and approved the submitted version.

***Possible AI Usage*:** Language tools helped with English wording and grammar during revision only. The authors completed the scientific content, data interpretation, and final approval, and they remain responsible for the work.

REFERENCES

1. Bergengren O, Pekala KR and Matsoukas K, *et al.* (2023) 2022 Update on Prostate Cancer Epidemiology and Risk Factors-A Systematic Review. *European Urology*, ***84****(2): 191-206.*
2. Chen W, Xu L, Deng H, Zhu Z and Yang D (2025) Role of USP10/ METTL3/CXCR4 Axis in Immunotherapy of Castration-Resistant Prostate Cancer. *Iran J Allergy Asthma Immunol*, ***24****(3):* 334-346.
3. Nayan M, Carvalho FLF and Feldman AS (2022) Active surveillance for intermediate-risk prostate cancer. *World Journal of Urology*, ***40*** *(1): 79-86.*
4. Liu S, Hsu E and Aslan M, *et al.* (2025) Extracellular Domain Shedding of TROP2 Activates EGFR Signaling to Drive Prostate Cancer Metastasis. *Cancer Research*, ***85****(23): 4632-4647.*
5. Carlsson SV and Vickers AJ (2020) Screening for Prostate Cancer. *The Medical Clinics of North America*, ***104****(6): 1051-1062.*
6. Sekhoacha M, Riet K, Motloung P, Gumenku L, Adegoke A and Mashele S (2022) Prostate Cancer Review: Genetics, Diagnosis, Treatment Options, and Alternative Approaches. *Molecules*, ***27*** *(17): 5730.*
7. Deng R, Liu Y and Wang K, *et al.* (2024) Comparison of MRI artificial intelligence-guided cognitive fusion-targeted biopsy versus routine cognitive fusion-targeted prostate biopsy in prostate cancer diagnosis: a randomized controlled trial. *BMC Medicine*, ***22****(1): 530.*
8. Dunn MW (2017) Prostate Cancer Screening. *Seminars in Oncology Nursing*, ***33****(2): 156-164.*
9. Merriel SWD, Funston G and Hamilton W (2018) Prostate Cancer in Primary Care. *Advances in Therapy*, ***35****(9): 1285-1294.*
10. Leslie SW, Soon-Sutton TL and Skelton WP: Prostate Cancer; StatPearls. Treasure Island (FL), StatPearls Publishing, 2026
11. Zhu Y, Shan J and Zhang Y, *et al.* (2019) Prostate Cancer Vascularity: Superb Microvascular Imaging Ultrasonography with Histopathology Correlation. *Medical Science Monitor*, ***25****: 8571-8578.*

[Downloaded from ijrr.com on 2026-11-15]

[DOI: 10.66224/ijrr.24.3.21]

12. Merriel SWD, Pocock L and Gilbert E, *et al.* (2022) Systematic review and meta-analysis of the diagnostic accuracy of prostate-specific antigen (PSA) for the detection of prostate cancer in symptomatic patients. *BMC Medicine*, ***20****(1): 54*.
13. Apfelbeck M, Clevert D, Ricke J, Stief C and Schlenker B (2018) Contrast enhanced ultrasound (CEUS) with MRI image fusion for monitoring focal therapy of prostate cancer with high intensity focused ultrasound (HIFU)1. *Clinical Hemorheology and Microcirculation*, ***69****(1-2): 93-100*.
14. Dias AB, O'Brien C, Correas J and Ghai S (2022) Multiparametric ultrasound and micro-ultrasound in prostate cancer: a comprehensive review. *The British Journal of Radiology*, ***95****(1131): 20210633*.
15. Gurwin A, Kowalczyk K and Knecht-Gurwin K, *et al.* (2022) Alternatives for MRI in Prostate Cancer Diagnostics-Review of Current Ultrasound-Based Techniques. *Cancers*, ***14****(8): 1859*.
16. Chen L, Xu Y and Wang Y, *et al.* (2024) Prostate cancer microenvironment: multidimensional regulation of immune cells, vascular system, stromal cells, and microbiota. *Molecular Cancer*, ***23****(1): 229*.
17. Maxeiner A, Fischer T and Schwabe J, *et al.* (2019) Contrast-Enhanced Ultrasound (CEUS) and Quantitative Perfusion Analysis in Patients with Suspicion for Prostate Cancer. *Ultraschall in Der Medizin (Stuttgart, Germany: 1980)*, ***40****(3): 340-348*.
18. Wildeboer RR, Postema AW, Demi L, Kuenen MPJ, Wijkstra H and Mischi M (2017) Multiparametric dynamic contrast-enhanced ultrasound imaging of prostate cancer. *European Radiology*, ***27****(8): 3226-3234*.
19. Postema AW, Gayet MCW and van Sloun RJG, *et al.* (2020) Contrast -enhanced ultrasound with dispersion analysis for the localization of prostate cancer: correlation with radical prostatectomy specimens. *World Journal of Urology*, ***38****(11): 2811-2818*.
20. Wildeboer RR, Mannaerts CK and van Sloun RJG, *et al.* (2020) Automated multiparametric localization of prostate cancer based on B-mode, shear-wave elastography, and contrast-enhanced ultrasound radiomics. *European Radiology*, ***30****(2): 806-815*.
21. Wildeboer RR, van Sloun RJG, Huang P, Wijkstra H and Mischi M (2019) 3-D multi-parametric contrast-enhanced ultrasound for the prediction of prostate cancer. *Ultrasound in Medicine and Biology*, ***45****(10): 2713-2724*.
22. Wegierak D, Cooley MB and Perera R, *et al.* (2024) Decorrelation time mapping as an analysis tool for nanobubble-based contrast enhanced ultrasound imaging. *IEEE Transactions on Medical Imaging*, ***43****(6): 2370-2380*.
23. Rebello RJ, Oing C and Knudsen KE, *et al.* (2021) Prostate cancer. *Nature Reviews Disease Primers*, ***7****(1): 9*.
24. Guo S, Kang F and Ma S, *et al.* (2024) The PRIMARY score: Diagnostic performance and added value compared with MRI in detecting clinically significant prostate cancer. *Clinical Nuclear Medicine*, ***49****(1): 37-44*.
25. Mei J, Zhao Y, Jiang Y, Wang J and Yu J (2020) Association between contrast-enhanced ultrasound indicators and prostate cancer biochemical recurrence after treatment. *Cancer Management and Research*, ***12****: 4959-4968*.
26. Yang F, Guo W, Sun S and Huang Y (2024) Diagnostic value of tripartite magnetic resonance imaging model based on T2-weighted imaging, diffusion-weighted imaging and dynamic contrast-enhanced imaging for prostatitis, prostatic hyperplasia and prostate cancer. *Int J Radiat Res*, ***22****(1): 111-116.*

[Downloaded from ijrr.com on 2026-11-15]

[DOI: 10.66224/ijrr.24.3.21]